Design of a 275-370 GHz SIS mixer with image sideband rejection and stable operation

A. Navarrini, D. Billon-Pierron, K.F. Schuster, B. Lazareff

IRAM (Institut de Radio Astronomie Millimétrique)

300, rue de la Piscine – 38406 St. Martin d'Hères -France

Abstract

We discuss the design and optimisation of a SIS Single Side Band (SSB) mixer covering the 275-370 GHz frequency band for astronomical applications. The junction is probe-coupled to the full height waveguide. An adjustable circular noncontacting backshort allows SSB tuning in either USB or LSB in the whole RF band. A ≈30 % operating bandwidth can be achieved by using parallel inductive tuning of the junction capacitance. The calculated SSB receiver noise temperature referred to the mixer input is in the range 25-38 K.

A stability criterion for an SSB mixer with distinct signal and image termination impedances under typical operating conditions is derived. We show that when an inductive series matching structure with a two-stage impedance transformer is used to compensate the junction capacitance, the mixer cannot be operated over a wide frequency range in a stable way. An inductive parallel matching structure with a single-stage transformer allows us to fulfill the necessary conditions of stability.

1 Introduction

Radio astronomical spectroscopy is the main driver for the development of low-noise heterodyne receivers in the mm and submm range. In a practical implementation on a telescope, the losses associated with infrared filtering, local oscillator injection, telescope spillover and atmospheric attenuation all contribute to degrade the actual figure of merit for astronomical spectroscopy: SSB system noise temperature. Referring the system noise to the mixer input, it can be expressed in a simplified form as:

$$T_{SSB} = G_S^{-1} \cdot (T_{out} + T_{IF}) + (1 + G_I / G_S) \cdot T_{in} \qquad (1)$$

where G_S and G_I are the coupled mixer gain in the signal and image band, T_{out} is the mixer noise temperature referred to its output, T_{IF} is the noise temperature of the IF amplifier and T_{in} is the input noise temperature including noise contributions from optics, spillover and sky. For a typical ground-based receiver, the second term is often

dominating the sum. Its impact can be minimized by realizing an SSB mixer. Another requirement is to cover the atmospheric transmission windows with a minimum number of distinct receivers; this is a driver for a wide tuning range of the mixer (and of the LO system). A third requirement is for stable operation to be achieved without critical tuning. Accordingly, our three main goals in the present work are: single sideband operation, wide RF tuning range, low noise and stable operation.

2 Full height waveguide to microstrip transition

The 275-370 GHz mixer waveguide (0.76×0.38 mm^2) supports single TE_{10} mode operation from 197 GHz to 394 GHz. To achieve a good match over the desired frequency band it is imperative that a probe impedance $Z_{ant}(\nu)$ is selected which can easily be tuned over the entire frequency range. A waveguide whose height is reduced relative to the normal b/a ratio is often used in SIS mixers to help achieve the impedance match between the waveguide and the junction. We found desirable to use a full-height waveguide (b/a=1/2) for two reasons : i) lower losses ; ii) easier transition to the circular section used for the backshort described in a later section.

Yassin and Withington [1] give analytical results for a transition from a full height waveguide to a TEM port, that achieves a very good match to a real, low impedance (20-50 Ω) over a full waveguide band, making it well suited for an SIS mixer. We used their results as a starting point for an optimization of the actual configuration, where the probe feeds a microstrip line, itself running atop a base metallization patterned as a choke to provide a virtual short at the waveguide entrance. The electromagnetic simulations, using the FDTD package Microwave Studio from CST [2], take into account the presence of the quartz substrate, the microstrip channel, and the first two sections of the suspended microstrip choke.

We adopted a substrate 250 μm wide, 80 μm thick, with 100 μm air below, and 50 μm air above. The placement of the probe perpendicular to the waveguide's E-plane (see Figs. 1, 3) allows to decouple the first non-TEM propagation mode of the suspended stripline, which otherwise would have required to decrease the substrate width to reject its cutoff above the operating frequency range, and resulted in a more delicate fabrication. The driving-point impedance at the base of the antenna, versus frequency (or versus backshort position) periodically returns through a fixed impedance Z_C, whose real and imaginary parts can be controlled by the probe angle and length, respectively (see Fig.1). Adopting L = 200 μm and $a = 90^0$ results in Z_C = 75 Ω. We find that a better broadband match can be obtained when the quartz substrate does not extend across the full width of the waveguide.

3 Circular non-contacting backshort

A mechanically rugged, noncontacting circular backshort has been adopted. Its role is to provide simultaneously a good match and a high mismatch at, respectively, the

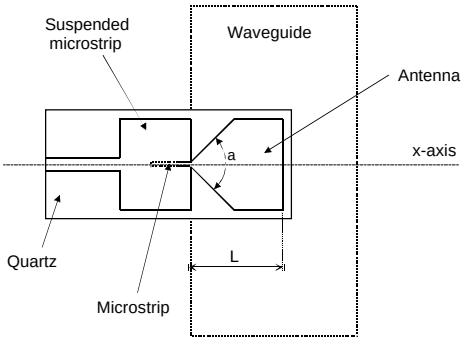

Fig. 1: Geometry of the probe transition from full-height waveguide to microstrip.

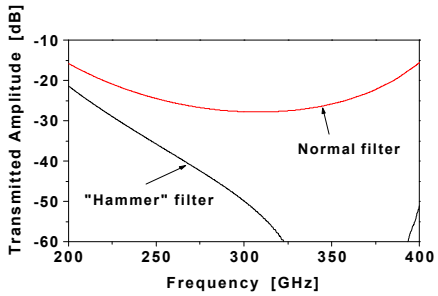

Fig. 2 : Amplitude of the transmission coefficient of six sections ²Hammer² type and normal type filter as a function of frequency.

signal and image frequencies; see sections 5 and 6 for a more complete discussion. It is located inside a circular waveguide of 880 µm diameter, and comprises 4 sections (Fig. 3). It has been optimized to provide a reflection coefficient better than -0.1dB across the operating band, taking into account imperfect contact of the rear part and a possible radial misalignment of 10 µm. For a given frequency range, the fabrication of a non-contacting backshort is easier in a circular (lathe) than in a rectangular (milling machine) waveguide, especially if the latter has reduced height. A conical transition between the rectangular and circular waveguide sections ensures that the reflected amplitude is dominated by the backshort itself, and ensures a regular tuning curve (see Fig. 7).

4 RF Filter

The base metallization on the quartz substrate is patterned into a six-section low-pass filter whose role is to provide a virtual short to the mixer block at the waveguide wall, and to reject the propagation of RF energy in the substrate channel. We found that a "hammer" type structure (visible on Figs 3 and 8) provides a superior rejection compared to the more common rectangular quarter-wave sections (see Fig. 2). A rectangular shape is kept for the first section to provide the space required for the microstrip tuning structures (section 7).

5 SSB Tuning

We start this section with an approximate, analytical discussion of SSB tuning. The principle of SSB operation is to locate the backshort so that its impedance in the plane of the waveguide to microstrip transition is an open at the signal frequency, and a short at the image frequency, which results in the junction being isolated from the mixer input and seeing a reactive termination at that frequency. Disregarding the fact that the

waveguide is non-uniform between the probe and the backshort, the shortest backshort distance that achieves that condition is such that:

$$l_{bs} = \tfrac{1}{2} n\, l_g(n_l) \quad \text{and} \quad l_{bs} = \tfrac{1}{2}(n+\tfrac{1}{2})\, l_g(n_u) \tag{2}$$

where we have assumed that the lower sideband is the image, and the upper sideband the signal. These two equations can be combined:

$$l_{bs} = \frac{1}{4(l_g^{-1}(n_u) - l_g^{-1}(n_l))} \approx \frac{c}{8n_{IF}} \sqrt{1 - \left(\frac{n_c}{n_{LO}}\right)^2} \tag{3}$$

This simple equation gives, for ν_{LO} = 300 GHz and ν_{IF} = 6 GHz, $l_{bs} \approx 4.6$ mm. We now discuss more detailed results from FDTD electromagnetic modeling. Figure 4 shows the driving point impedance $Z_P(\nu)$ of the probe, in the range 275–370 GHz, for a backshort distance from the probe $l_{bs} \approx 8$ mm. Z_P describes a circle, that slowly sweeps around the Smith chart. At periodic intervals, Z_P passes through a fixed point of real impedance Z_C = 75 Ω, for which the probe was optimized, and, halfway through each rotation, Z_P touches the circle $\Gamma = 1$. For a different value of l_{bs}, the rate of rotation, and the total number of loops between 275–370 GHz, would be different, but the general region swept in the Smith chart would remain the same.

At this point, one might believe that all is needed is a suitable circuit to match the junction to Z_C, a problem for which several solutions are well known. We must, however, pay attention to the stability of the mixer operating in the SSB mode, which will be addressed in the two next sections.

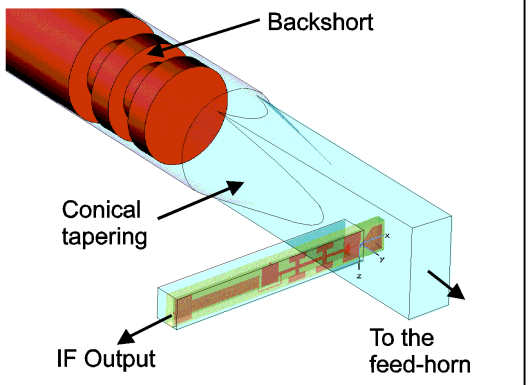

Fig. 3 : Full height waveguide SSB mixer. The circular section backshort is used for image rejection.

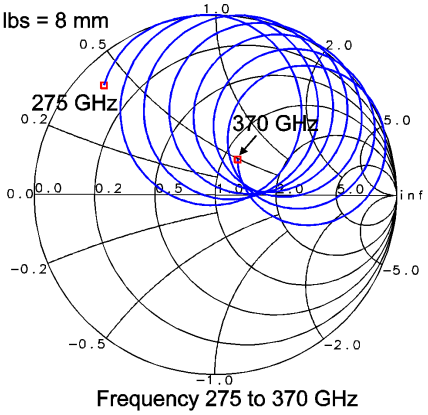

Fig. 4 : Driving point impedance of the probe for the mixer geometry shown in Figs.3 and 8 : The circular backshort is located at a distance l_{bs}=8mm away from the antenna plane. The Smith chart is normalised to 50 W.

6 Stability of SSB Mixer

In this section, we use Tucker's theory of quantum mixing [3] to derive a stability criterion for a SSB mixer operating in the 275-370 GHz range. We use the three-port approximation, treating only signals at $\nu_m = \nu_{LO} + m\,\nu_{IF}, m = 0,\pm 1$ and assuming higher harmonics to be shorted out by the junction capacitance. The geometry of the waveguide mount and the tuning circuit (including the junction's geometric capacitance) define the admittances seen by the junction at the three frequencies ν_m. Note that in the present case, $Y_{-1} \neq Y_1^*$. The dimensionless LO amplitude α defines the conversion matrix $Y_{mn}, m,n = 0,\pm 1$; we use the results and notations of Tucker and Feldman [4]. From these one can compute the augmented *Y* matrix and its inverse *Z*. The output IF admittance of the mixer is given by:

$$Y_{IF} = Z_{00}^{-1} - Y_0 \qquad (4)$$

It is physically clear (although slightly less obvious from the algebra) that Y_{IF} is independent of Y_0, and represents the IF output impedance of the mixer, when the RF ports are terminated at definite impedances, and for a given LO pumping level.

For a purely DSB mixer ($Y_{-1} = Y_1^*$), including the case of zero IF, Y_{IF} is real and equal to the slope of the pumped I-V curve. These two conditions do not hold any more in the general case [5]. The stability condition when the mixer's IF output is connected to a load Y_0 can be written: $\mathrm{Re}(Y_{IF}) + \mathrm{Re}(Y_0) > 0$. For the mixer to be stable for an arbitrary passive load, we require: $\mathrm{Re}(Y_{IF}) > 0$. The optimum operating conditions for a SSB mixer have been discussed by L.R. D'Addario [6]. In the present work, we have restricted the parameter space by assuming that the bias voltage is at the middle of the first photon step, $V_{DC} = V_g - hn_{LO}/2e$, and that the normalized pump voltage is unity: $\alpha = eV_{LO}/h\nu_{LO} = 1$; such parameters usually result in near-optimum noise performance. Moreover, we have assumed Z_S to match the normal-state resistance of the junction R_n, $Z_S = R_n$, and Z_I to be purely reactive ($Z_I = j\cdot X$ with X arbitrary reactance) which implies that the image band is completely rejected. Using an analytic fit to the I-V curve at 4.2 K of a good quality junction, we have used a three-frequency approximation to the quantum theory of mixing to constrain the Z_I values necessary to ensure $\mathrm{Re}[Y_{IF}] > 0$. We find that the lowest frequency in the range, 275 GHz, constrains the limits of the "stability region" :

$$-3.27 \leq \frac{Z_I}{jR_n} \leq +0.12 \qquad (5)$$

The stability region derived in eq. (5) is plotted in Figs. 5 and 6 in a Smith chart normalised to R_n.

7 RF Matching Circuit

The 1 μm^2 Nb/Al-AlO_x/Nb junction has a critical current density of the order of 10 kA/cm^2 and a normal-state resistance R_n = 25 Ω [7]. It has been realised by e-beam lithography. The small-signal impedance of the tunnel barrier $R_{RF} = G_{11}^{-1}$ is, at the center frequency of 320GHz, $R_{RF} \approx 0.72 R_N \approx 18\Omega$. The parallel combination of R_{RF} and the junction capacitance, estimated to be 75 fF ($\omega RC \approx 2.7$), must be matched, at the signal frequency, to the impedance of the waveguide probe. Two of the most common means to achieve this are series inductive tuning (end-loaded stub) and parallel inductive tuning.

In the rest of this section, we first show that a matching circuit comprising an end-loaded stub and a two-section quarter wave transformer does not allow to meet the criterion for stable SSB operation; then we discuss the results obtained with parallel inductive tuning.

7.1 End-loaded stub with two-section transformer

Impedance matching by an end-loaded stub has been discussed by several authors [8]. The end-loaded stub puts a small section transmission line in series with the junction. This results in the transformation of the complex junction impedance to a purely real impedance

$$R_S \approx \frac{R_j}{2 \cdot (w R_j C)^2} \approx 1.2\ \Omega \qquad (6)$$

Matching such a relatively low R_S value to the 75 Ω antenna probe requires a two-section quarter-wave Chebyshev transformer. All transmission lines are implemented in superconducting microstrips with their lines and ground planes made of Nb (120 nm and 430 nm respectively) separated by a 200 nm thick insulating layer of SiO_2 ($\varepsilon_R \cong 4.3$). The widths and lengths of the transmission lines have been optimised for maximum coupling of the RF junction resistance to the antenna probe in the 275-370 GHz frequency range using a commercial software (HP-EEsof Series IV EEsof, Libra-Touchstone), with appropriate corrections for field penetration.

The Smith chart (Fig. 5) shows the embedding impedance $Z_{emb}(\nu)$ in the 275-370 GHz frequency band for a backshort position l_{bs} = 8 mm (increased for clarity) away from the antenna plane. At alternate frequencies, the junction sees a match and a reactive mismatch, respectively, as required for SSB operation. However, the reactive termination at the image frequency lies, in some cases, in the region of instability; this is due to the phase dispersion caused by the two quarter-wave sections of the transformer. This matching circuit must be rejected.

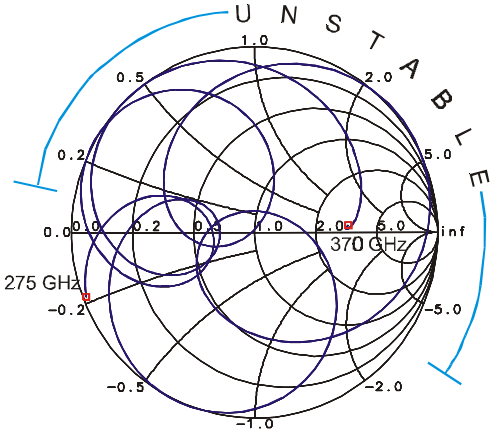

Fig. 5 : Series inductive tuning with two-section l/4 transformer. Impedance seen by the junction. Note that the reactive termination used for image rejection lies, in some cases, in the "unstable" region. The Smith chart is normalised to $Z_S=R_n$.

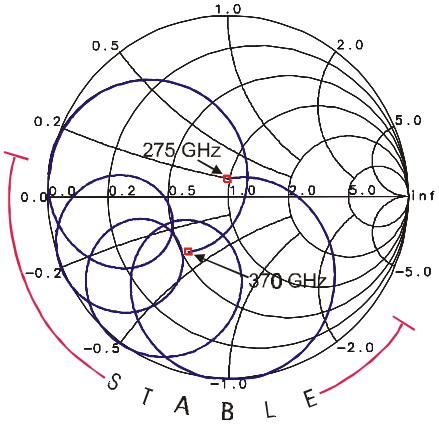

Fig. 6: Parallel inductive tuning with single-section l/4 transformer. Impedance seen by the junction. The reactive termination used for image rejection is always within the "stable" region. Here the backshort distance is 4.2 mm, appropriate for USB operation at 320 GHz.

7.2 Parallel inductive tuning with single-section transformer

A better control of this impedance is obtained by using a lower value for the electrical length between the antenna probe and the junction. This is achieved by adopting a parallel inductive tuning. The required transformation ratio is smaller and can be achieved with a single section λ/4 transformer. The layout of the mixer chip is illustrated in Fig. 8. The parallel inductive tuning is achieved with a short (≈λ/8) length of microstrip, terminated to a virtual ground provided by a radial stub (opening angle 130^0). We found, using simulations [9], that, with respect to the conflicting requirements of lowest impedance at the apex on one hand, and minimum capacitive loading of the IF on the other hand, a radial stub offers no clear advantage over a λ/4 low-impedance rectangular stub. The parallel tuned junction presents, at the centre of the RF band, a real impedance $R_j \approx 18\ \Omega$ as discussed above. This is matched to the ≈ 75 Ω driving point impedance of the probe by a λ/4 line with an impedance $Z_L \approx 35\ \Omega$. This falls between the impedances that can be realised in, respectively, microstrip and coplanar superconductive lines. We have realised this λ/4 section in Capacitively Loaded CoPlanar Waveguide (CLCPW), consisting of 3 sections of microstrip and 2 sections of coplanar lines.

The lengths of the individual sections were optimised, taking into account the actual impedances across the RF band of the inductively tuned junction and of the probe, while ensuring at the same time that the stability criterion for SSB operation was met. Sonnet ***em*** was used to compute de-embedded S-parameters for the microstrip-

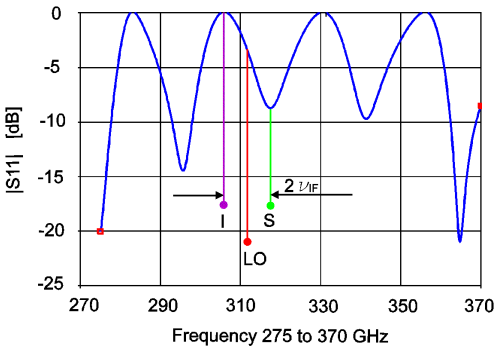

Fig. 7 Amplitude of the reflection coefficient |S11(n)| seen by the junction.

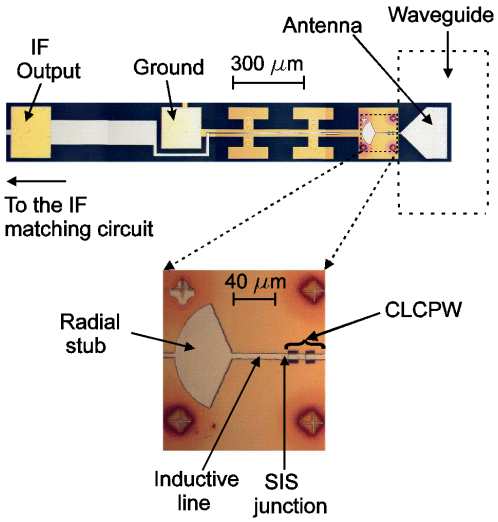

Fig. 8: Quartz substrate used for the mounting of the SIS junction and the integrated tuning structure

coplanar discontinuities, which were used in the Libra simulation of the global circuit. The final result of the optimisation is shown in Figs. 6 and 7.

8 Junction bias and IF Matching Circuit

To bias the junction and provide a path for the IF signal, a narrow microstrip line (3 μm) is connected to the external part of the radial stub as shown in Fig. 8 using alternate $\lambda/4$ sections to reject RF leakage.

9 Modelling results: Gain and mixer noise temperature

Using the standard quantum theory of mixing in the three-port approximation, we have computed the coupled mixer gain, the image band rejection, the SSB mixer noise temperature and the SSB receiver noise temperature of our designed system. We assumed a noise temperature of the IF amplifier $T_{IF}=6\,K$. We also assumed a bias voltage at the half of the first photon step and a LO pumping power such that $\alpha=1$. The receiver has been optimised for SSB operations by tuning the backshort distance from the antenna plane l_{bs} to allow operations with low G_I/G_S in either USB or LSB at each frequency in the RF band. Fig. 9 shows the estimated SSB *mixer* noise temperature T_M and the coupled signal mixer gain G_S. This result shows that the mixer can operate with low mixer noise temperature and reasonable signal conversion gain. Fig. 10 shows the calculated SSB *receiver* noise temperature and the backshort to antenna plane distance l_{bs} expressed in mm required for the SSB tuning. We can see that a worst-case $T_{rec} \approx 38$ K ($\approx 2.4\ h\cdot\nu/k$) occurs at 330 GHz. The result shown in

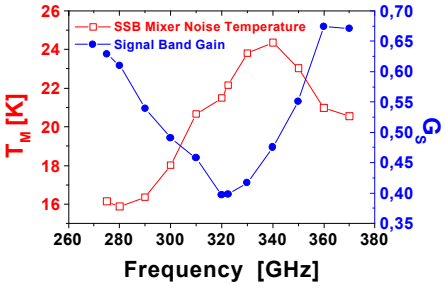

Fig. 9: Calculated SSB mixer noise temperature and coupled mixer gain in the signal band G_S (linear scale) in the 275-370 GHz frequency band.

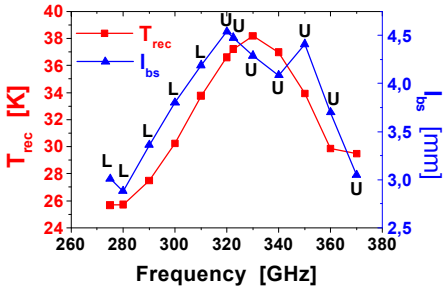

Fig. 10: Calculated SSB receiver noise temperature T_{rec} and backshort in the 275-370 GHz frequency band, in LSB (L) or USB (U).

Fig. 10 indicates that a SSB receiver noise temperature as low as ≈ 2÷3 times the quantum limit hν/k might be achieved over the whole 275-370 GHz frequency band.

10 Mixer block construction

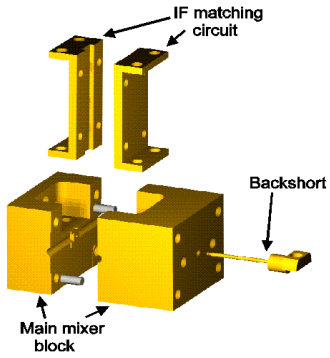

Fig. 11: Mixer block configuration: the two main parts of the mixer used for the SIS junction mounting are shown together with the circular section backshort and the shielded microstrip used as IF matching transformer.

The main mixer block is split in two parts, which are machined in brass. The mixer block includes magnetic field concentrators for the suppression of the Josephson current. The whole device is illustrated in Fig. 11. Here the two main parts of the mixer are shown together with the circular section backshort and the shielded microstrip used as IF matching transformer. The main mixer block has external dimensions $25 \times 20 \times 25$ mm^3. One part of the mixer includes the circular waveguide, housing the backshort, the conical transition circular to rectangular waveguide and a short section of rectangular waveguide. This part of the mixer is used for SIS junction mounting. The other part of the main block includes a 10 mm long rectangular waveguide which has been realised by spark erosion technique. The other parts of the block have been micromachined in a standard way.

11 Conclusions

A new type of SIS heterodyne quasi-particle mixer has been designed for the 275-370 GHz band. The mixer employs a tuned junction mounted in a full height waveguide block and a circular section backshort used for SSB operations. The RF matching network consists of an open-ended stub including a radial stub and an inductive microstrip line. The mixer and its external circuit have been optimised to give wide RF

bandwidth, low mixer noise temperature and high gain. SSB mixer noise temperatures in the range 16-25 K are expected in the RF band with a mixer conversion gain better than -4.0 dB. SSB receiver noise temperatures are in the range 25-38 K in the same frequency band.

Acknowledgements

The authors are grateful to M. Carter and F. Mattiocco for helpful discussions. I. Peron played in crucial role in developing the E-beam lithography in IRAM's SIS laboratory. This work was supported in part by the Institut de Radio Astronomie Millimétrique IRAM (Grenoble, France), and by the CNAA, Astrophysical Observatory of Arcetri (Florence, Italy).

References

[1] G. Yassin and S. Withington, "Analytical Expression for the Input Impedance of a Microstrip Probe in Waveguide", *Int. J. Infrared and Millimetre Waves*, **17**, 1685-1705, 1996

[2] CST Microwave Studio, Büdinger Str. 2 a, D-64289 Darmstadt, Germany

[3] J.R. Tucker, "Quantum limited detection in tunnel junction mixers", *IEEE J. Quantum Electron.*, **6**, 1234-1258, 1979

[4] J.R. Tucker and M.J. Feldman, "Quantum detection at millimetre wavelengths", *Rev. Mod. Phys.,* **57,** 1055-1113, 1985

[5] S.-K. Pan and A.R. Kerr, "SIS mixer analysis with non-zero intermediate frequencies", *Seventh International Symposium on Space Terahertz Technology*, Charlottesville, March, 1996

[6] L. D'Addario, "Noise Parameters of SIS Mixers", *IEEE Trans. Microwave Theory and Techniques*, **36**, (7), 1196-1206, 1988

[7] K.F. Schuster, IRAM Technical Memo, 1998

[8] T.H. Büttgenbach, H.G. LeDuc, P.D. Maker, T.G. Phillips, "A Fixed Tuned Broadband Matching Structure for Submillimetre Astronomy ", *IEEE Trans. Applied Supercond.*, **2**, (3), 165-175, 1992

[9] Sonnet Software, Inc., 1020 Seventh North Street, Suite 210, Liverpool, NY 13088, USA